NeuroImage **16,** 1151–1155 (2002)
doi:10.1006/nimg.2002.1119

RAPID COMMUNICATION

Reduction of Gradient Acoustic Noise in MRI Using SENSE-EPI

Jacco A. de Zwart,* Peter van Gelderen,* Peter Kellman,† and Jeff H. Duyn*

**Advanced MRI, Laboratory of Functional and Molecular Imaging, NINDS; and †Laboratory of Cardiac Energetics, NHLBI, National Institutes of Health, Bethesda, Maryland*

Received December 14, 2001

A new approach to reduce gradient acoustic noise levels in EPI experiments is presented. Using multichannel RF receive coils, combined with SENSE data acquisition and reconstruction, gradient slew-rates in single-shot EPI were reduced fourfold for rate-2 and ninefold for rate-3 SENSE. Multislice EPI experiments were performed on three different scanner platforms. With 3.4 mm in-plane resolution, measuring 6 slices per second (12 slices with 2000 ms TR), this resulted in average sound pressure level reductions of 11.3 dB(A) and 16.5 dB(A) for rate-2 and rate-3 SENSE, respectively. BOLD fMRI experiments, using visually paced finger-tapping paradigms, showed no detrimental effect of the acoustic noise reduction strategy on temporal noise levels and *t* scores.

INTRODUCTION

In MRI, acoustic noise is generated when gradients are switched, which results in changing Lorentz forces on the gradient coil conductor (Mansfield *et al.*, 1998). Echo Planar Imaging (EPI) (Mansfield and Pykett, 1978), a popular technique for functional magnetic resonance imaging (fMRI), generates high levels of gradient acoustic noise, particularly when used at high image resolution. The oscillatory switching patterns characteristic for EPI techniques drive an often intense spectrum of acoustic frequencies in the human auditory range. This can cause discomfort and distress for anyone inside or in the vicinity of the magnet, and ultimately pose an upper limit to the practically usable gradient slew rates and field strengths for EPI. Furthermore, in fMRI, subject discomfort and exposure to acoustic noise can interfere with the experiment and affect the brain activation under study (Cho *et al.*, 1998; Shah *et al.*, 2000). This could be specifically problematic in studies of the auditory system, imposing restrictions on the design of the activation paradigm (Belin *et al.*, 1999; Eden *et al.*, 1998).

There is a number of ways to reduce the sound pressure level (SPL) in MRI. These include modifications of the gradient coil design (Mansfield *et al.*, 1995, 2001), the mechanical characteristics of the gradient former, and specific mounting or packing and padding strategies of the gradients. In addition, sound-absorbing material can be attached to reflecting surfaces such as the cryostat and the scan room walls, ceiling and floor. At the patient, SPL reduction can be achieved by sound dampening devices such as earplugs and earphones, or by an active sound cancellation system (Goldman *et al.*, 1989; McJury *et al.*, 1997). Furthermore, SPL can be reduced by specific design of shape and timing of the gradient waveforms (Hennel *et al.*, 1990). In this report, we propose the use of sensitivity encoding (SENSE) technology (Pruessmann *et al.*, 1999) to reduce SPL in BOLD fMRI through slew-rate reduction. In combination with multi-element detector arrays, SENSE allows reduction of gradient switching through reduced sampling of *k*-space, leading to a reduced field-of-view (FOV) in the acquired image. Aliasing artifacts are removed in post-processing by incorporating prior knowledge about B_1-field distributions of the coil elements in the image reconstruction. Preliminary studies have demonstrated the feasibility of applying SENSE in fMRI to shorten the image acquisition time (Golay *et al.*, 2000) and/or improve spatial resolution in BOLD fMRI at constant slew-rate (de Zwart *et al.*, 2001; de Zwart *et al.*, submitted). In the following, gradient slew-rate reduction was achieved at constant image acquisition time and resolution.

MATERIALS AND METHODS

MRI experiments were performed on 1.5 T and 3.0 T GE Signa LX scanners (General Electric Company, Milwaukee, WI), both with cardiac resonator module (CRM) gradients ($40\ \mathrm{mT \cdot m^{-1}}$, $180\ \mathrm{T \cdot m^{-1} \cdot s^{-1}}$), and a 1.5 T Siemens Magnetom scanner (Siemens Medical Systems, Erlangen, Germany) with Sonata gradients ($40\ \mathrm{mT \cdot m^{-1}}$, $200\ \mathrm{T \cdot m^{-1} \cdot s^{-1}}$). EPI with internal

1053-8119/02

phase reference (Bruder *et al.*, 1992; Yang *et al.*, 1998) was performed using 40 ms TE, 2000 ms TR and 90° flip angle. For full *k*-space imaging (without SENSE acceleration), 12 4-mm-thick axial slices were collected with 1 mm interslice gap, 220×165 mm^2 FOV, matrix size 64×48 (anterior-posterior × left-right) and 4 μs dwell time. The EPI read-gradient, applied in the anterior-posterior direction, consisted of trapezoidal waveforms with flat portions of 124 μs and ramps of 180 μs duration, and a maximum amplitude of 26.7 $\mathrm{mT \cdot m^{-1}}$. This corresponds to maximum slew rates of 148.3 $\mathrm{T \cdot m^{-1} \cdot s^{-1}}$. Slew-rates of other gradient waveforms, such as the blipped phase-encode gradient, the slice selection gradients, and crusher gradients, were all well below 150 $\mathrm{T \cdot m^{-1} \cdot s^{-1}}$. The total duration of the EPI readout window, including acquisition of an additional echo used for phase correction, was 23.8 ms. Fifty percent of the ramps of the readout gradient was used for data sampling. Phase-encode blips were positioned on the remaining part of the readout gradient.

Rate-2 (2-fold undersampled) SENSE MRI (Pruessmann *et al.*, 1999) was performed in the left-right direction using a FOV of 220×83 mm^2, a matrix size of 64×24 (reconstructed to 220×165 mm^2 FOV and 64×48 matrix size, respectively), and a dwell time of 8 μs. Compared to full *k*-space EPI, the readout gradient amplitude was reduced 50% to 13.4 $\mathrm{mT \cdot m^{-1}}$, and the readout gradient ramp time was doubled to 360 μs, resulting in a maximum slew rate of 37.1 $\mathrm{T \cdot m^{-1} \cdot s^{-1}}$. The acquisition time of the SENSE *k*-space matrix was identical to that of the full *k*-space matrix, however the total duration of the EPI train was slightly longer (24.6 ms) due to the acquisition of the internal phase reference line (49 echoes were acquired in conventional EPI, 25 echoes in rate-2 SENSE). For the SPL measurements, SENSE EPI was also performed at a SENSE rate of 3 (64×16 acquired matrix size, 12 μs dwell time), resulting in a maximum readout gradient strength of 8.9 $\mathrm{mT \cdot m^{-1}}$, and a maximum slew-rate of 16.5 $\mathrm{T \cdot m^{-1} \cdot s^{-1}}$, which was one-ninth of the slew-rate of the full FOV acquisition. SENSE image reconstruction was performed as described earlier (Pruessmann *et al.*, 1999). Acoustic noise levels were measured in front of the scanner using a Sper Scientific (Sper Scientific Ltd., Scottsdale, AZ) sound pressure level meter, model 840029. The meter was used on A-scale weighting and "slow" response settings, the latter referring to the integration time. The A-weighted dB-scale is a standardized measure for SPL, which accounts for the frequency response of the human ear. It is a logarithmic value, relative to a reference noise level, for which typically $2.0 \cdot 10^{-5}\ \mathrm{N \cdot m^{-2}}$ is used (an approximation for the lower hearing threshold for the average youth):

$$\mathrm{dB(A)} \propto 20 \cdot \log(P/P_r), \qquad (1)$$

where P is the measured SPL, and P_r the reference sound pressure level. An SPL-increase of 20 dB(A) is perceived as a 10-fold increased loudness. The meter was positioned approximately on-axis with the magnet, at about 3.5 m from magnet isocenter. This distance was chosen to minimize interference of the static field with the performance of the sound level meter. SPL measurements were performed with a 2-liter spherical phantom positioned in the head coil and with a foam pad for patient support in place. To determine the contribution of gradients other than the readout train on SPL, conventional EPI was also performed with the amplitude of the readout gradients set to zero.

The fMRI sensitivity of conventional and SENSE EPI was compared in motor cortex activation studies. These experiments were performed with informed consent on the 1.5 T GE scanner on six normal volunteers, both male and female, ranging in age from 23.1 to 35.7 years (28.6 years on average), in accordance with an NIH-approved protocol (IRB approval number: 00-N-0082; last reviewed: March 29, 2002). A four-channel, dome-shaped head coil (Nova Medical Inc., Wakefield, MA) of gapped-element design (Ledden and Inati, 2001) was used for signal reception. A sequential finger-tapping activation paradigm, visually paced at 2 $\mathrm{taps \cdot s^{-1}}$ (2 Hz), was used with 5 alternating rest and active stages of 30 s each. The paradigm was started after an initial (setup) scan period of 60 s.

Four fMRI runs were performed per subject, with two full *k*-space and two SENSE acquisitions performed in random order (on one of the volunteers only a single pair of data was acquired). In the SENSE fMRI experiments, on alternate time points, only even *k*-space lines (the lines 0, 2, 4, . . . of the corresponding full *k*-space) or odd lines (the lines 1, 3, 5, . . . of the corresponding full *k*-space) were measured (Kellman *et al.*, 2001). To derive coil sensitivity reference maps, full FOV images were reconstructed from two successive time-points and averaged. The first 10 time-points were discarded to ensure a steady-state condition for the MR signal. Object intensity and phase contrast were removed from the reference data using respectively a root-sum-of-squares (RSS) combined magnitude image and an RSS-weighted combined phase image (de Zwart *et al.*, submitted). These steps were taken to remove high frequency phase and spatial signal intensity fluctuations, related to the object, which would negatively affect spatial smoothing and extrapolation of these relative coil sensitivity data. Note that the resulting images contain information about the relative differences in coil sensitivity, not absolute coil sensitivity, since no external reference (e.g., using a body coil image (Pruessmann *et al.*, 1999)) was used.

Following image registration (Thévenaz *et al.*, 1995), a quantitative measure of fMRI sensitivity was obtained by statistical analysis of the time-series data. For this purpose, multilinear regression was per-

TABLE 1

Gradient Acoustic Noise Levels on Three Scanner Platforms for Conventional EPI and SENSE EPI

	EPI acoustic noise level [dB(A)]			
MRI platform	Conventional	Readout off	Rate-2 SENSE	Rate-3 SENSE
1.5 T GE Signa LX	89.1	71.7	75.1	70.2
3.0 T GE Signa LX	87.7	72.6	75.7	72.9
1.5 T Siemens Sonata	91.3	74.5	83.5	75.6

Note. "Readout off" is the acoustic noise level measured in conventional EPI when readout gradients were turned off.

formed using four regressors: the stimulus function convolved with a hemodynamic response function; baseline intensity; a linear drift term; a "saw-tooth" function describing the possible signal intensity fluctuations in SENSE data (due to acquisition of "odd" or "even" lines on alternate time points). The hemodynamic response function was modeled as a truncated Gaussian function, delayed 5 s from the activation paradigm (Waldvogel *et al.*, 2000). The regression analysis returned statistical *t* scores, as well as the standard deviation of the difference between data and fit. The latter was used as a measure of temporal noise of the image intensity time course, in the following referred to as TSD.

For each subject, a single region-of-interest (ROI) in the primary motor cortex (PMC) area was selected based on anatomy. Voxels within this ROI, and with *t* values above 4.5 in any of the runs, were used to generate a "functional" PMC ROI (FPMC), over which *t* scores and TSD values were averaged.

RESULTS AND DISCUSSION

Table 1 shows the results of the SPL measurements during full *k*-space and SENSE EPI. SPL reductions with SENSE were substantial on all scanners and averaged 11.3 dB(A) and 16.5 dB(A) for rate-2 and rate-3 SENSE, respectively. The changes in SPL with SENSE are attributed primarily to the reduction in slew rate and gradient amplitude of the EPI readout gradient. A secondary effect of the application of SENSE was a change in pitch of the gradient sound due to increased echo spacing. This might also have affected the measured SPL levels. Eliminating the readout gradient resulted in SPL levels similar the levels obtained with rate-3 SENSE. Further reductions in SPL are expected for SENSE EPI performed at higher acceleration rates, or when using non-linear gradient ramps (e.g., sinusoidal). The SPL induced by the non-readout gradients in the conventional EPI sequence was assessed by turning off all read-out gradients and resulted in an average SPL-reduction of 16.4 dB(A).

Interestingly, the 3.0 T SPL values were not much higher than the 1.5 T values, as would have been expected based on the twofold increased Lorentz forces at 3.0 T. Possible explanations are the differences in cryostat geometry, coil mounting and scan room layout and furnishing. These differences, as well as differences in gradient coil geometry, could also explain the higher SPL levels found with the Siemens 1.5 T as compared to the GE 1.5 T.

Fig. 1 shows an example of fMRI data obtained with full *k*-space and SENSE acquisitions. Both methods show very similar results, confirming the feasibility of our acoustic noise reduction strategy. A more comprehensive evaluation is show in Table 2, which summarizes the SENSE and full *k*-space *t* scores and TSD levels for the fMRI studies performed on six subjects. Average signal-to-noise ratio (SNR) in FPMC was 190.5, corresponding to an intrinsic noise level (ISD) of 0.52%. One pair of data was excluded on the basis of TSD, since TSD exceeded a threshold of 4 times ISD, suggesting significant motion that was not corrected for by image registration (confirmed by visual inspection of the data). No significant difference between SENSE and full *k*-space was found. The *t* scores averaged, respectively, 5.59 for conventional EPI and 5.81 for SENSE-EPI, and TSD levels averaged 1.37% and 1.29%, respectively. Noise amplification resulting from the SENSE image reconstruction is typically expressed as the SENSE *g*-factor (Pruessmann *et al.*, 1999). The *g*-factors are spatially varying and depend amongst others on coil configuration and SENSE reduction factor. In the experiments described here, the average *g*-factor in PMC was 1.04; a small (4%) increase in TSD would therefore be expected. On the other hand, TSD in SENSE might benefit from reduced motion sensitivity because of the reduced gradient switching and lower-amplitude gradients, which will reduce phase accumulation effects caused by tissue motion during EPI-readout.

The similarity in TSD levels suggests that the sensitivity to detect brain activation is not significantly altered with the current application of SENSE. On the other hand, conventional applications of SENSE to reduce image distortions and blurring (Bammer *et al.*, 2001) or increase spatial resolution (de Zwart *et al.*, submitted) are likely to substantially increase TSD due to reduction in image SNR by a factor up to $g \cdot \sqrt{R}$ for a given spatial resolution (Pruessmann *et al.*, 1999), where R is the SENSE acceleration rate. The similarity in average *t* scores in FPMC indicates that brain activation was not significantly different with the altered data acquisition scheme and lower SPL level of SENSE. This finding might be task-dependent (Cho *et al.*, 1998) and does not necessarily transfer to other activation paradigms and experimental conditions. fMRI studies with non-EPI techniques found constant activation levels (Elliot *et al.*, 1999) or significant acti-

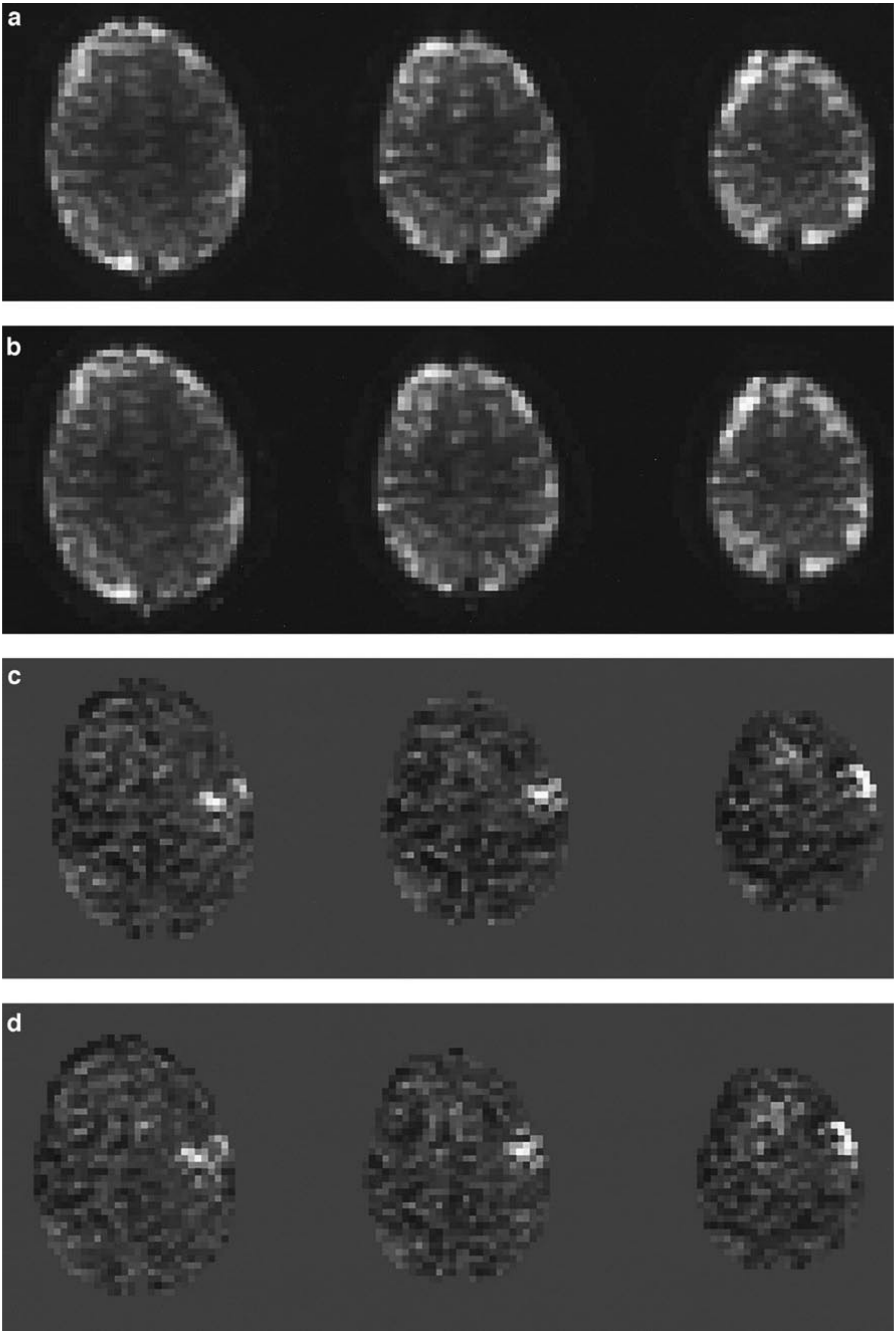

FIG. 1. Comparison of a motor cortex activation study performed with conventional EPI and with reduced gradient acoustic noise using SENSE. Baseline intensity (a, b) or *t* score (c, d) are not substantially altered with SENSE (b, d) compared to conventional (a, c) EPI, while SPL was reduced 14.0 dB(A) on this platform. Statistical *t* maps were scaled from −10 to +15.

TABLE 2

Comparison of *t* Scores and Temporal Instability [TSD, %] between Conventional and SENSE fMRI, Optimized for Acoustic Noise Reduction

	t scores		TSD	
Volunteer	Full	SENSE	Full	SENSE
1	8.69	7.99	1.27	1.47
2A	3.53	7.37	1.39	0.81
2B	6.97	7.01	0.90	0.88
3A	9.41	4.31	1.36	1.87
4A	7.14	6.56	1.36	1.77
4B	6.77	7.72	1.55	1.47
5A	3.04	2.27	1.67	1.36
5B	4.90	4.15	1.58	1.10
6A	2.60	5.37	1.42	0.99
6B	5.82	5.38	1.17	1.15
Average	5.59 (2.53)	5.81 (1.85)	1.37 (0.22)	1.29 (0.36)

vation increases (Cho *et al.*, 1998; Loenneker *et al.*, 2001) with SPL reduction in somatosensory stimulation in humans, whereas another study in anesthetized animals (Burke *et al.*, 2000) found activation decreases. It is expected that studies of the auditory system will benefit from SPL reduction due to reduced interference with activation paradigm. In summary, the reduction of acoustic noise levels available with SENSE-EPI allows improved subject comfort and improved presentation of the activation paradigm. The noise reduction obtainable with SENSE is not limited to EPI-fMRI, but can also be extended to other scan protocols, including those used for anatomical MRI.

ACKNOWLEDGMENT

Dr. Alan Koretsky is acknowledged for helpful discussions.

REFERENCES

Bammer, R., Keeling, S. L., Augustin, M., Pruessmann, K. P., Wolf, R., Stollberger, R., Hartung, H.-P., and Fazekas, F. 2001. Improved diffusion-weighted single-shot echo-planar imaging (EPI) in stroke using sensitivity encoding (SENSE). *Magn. Reson. Med.* **46:** 548–554.

Belin, P., Zatorre, R. J., Hoge, R., Evans, A. C., and Pike, B. 1999. Event-related fMRI of the auditory cortex. *Neuroimage* **10:** 417–429.

Bruder, H., Fischer, H., Reinfelder, H.-E., and Schmitt, F. 1992. Image reconstruction for echo planar imaging with nonequidistant *k*-space sampling. *Magn. Reson. Med.* **23:** 311–323.

Burke, M., Schwindt, W., Ludwig, U., Hennig, J., and Hoehn, M. 2000. Facilitation of electric forepaw stimulation-induced somatosensory activation in rats by additional acoustic stimulation: An fMRI investigation. *Magn. Reson. Med.* **44:** 317–321.

Cho, Z.-H., Chung, S.-C., Lim, D.-W., and Wong, E. K. 1998. Effects of the acoustic noise of the gradient systems on fMRI: A study on auditory, motor, and visual cortices. *Magn. Reson. Med.* **39:** 331–336.

Eden, G. F., Joseph, J. E., Brown, H. E., Brown, C. P., and Zeffiro, T. A. 1999. Utilizing hemodynamic delay and dispersion to detect fMRI signal change without auditory interference: The behavior interleaved gradients technique. *Magn. Reson. Med.* **41:** 13–20.

Elliot, M. R., Bowell, R. W., and Morris, P. G. 1999. The effect of scanner sound in visual, motor and auditory functional MRI. *Magn. Reson. Med.* **41:** 1230–1235.

Golay, X., Pruessmann, K. P., Weiger, M., Crelier, G. R., Folkers, P. J. M., Kollias, S. S., and Boesinger, P. 2000. PRESTO-SENSE: An ultrafast whole-brain fMRI technique. *Magn. Reson. Med.* **43:** 779–786.

Goldman, A. M., Gossman, W. E., and Friedlander, P. C. 1989. Reduction of sound levels with antinoise in MR Imaging. *Radiology* **173:** 549–550.

Hennel, F., Girard, F., and Loenneker, T. 1999. “Silent” MRI with soft gradient pulses. *Magn. Reson. Med.* **42:** 6–10.

Kellman, P., Epstein, F. H., and McVeigh, E. R. 2001. Adaptive sensitivity encoding incorporating temporal filtering (TSENSE). *Magn. Reson. Med.* **45:** 846–852.

Ledden, P. J., and Inati, S. 2001. Four channel preamplifier decoupled phased array for brain imaging at 1.5T. *Proc. Int. Soc. Magn. Reson. Med.* **9:** 1117. [Abstract]

Loenneker, T., Hennel, F., Ludwig, U., and Hennig, J. 2001. Silent BOLD imaging. *Magn. Reson. Materials Phys. Biol. Med.* **13:** 76–81.

Mansfield, P., Haywood, B., and Coxon, R. 2001. Active acoustic control in gradient coils for MRI. *Magn. Reson. Med.* **46:** 807–818.

Mansfield, P., Glover, P. M., and Beaumont, J. 1998. Sound generation in gradient coil structures for MRI. *Magn. Reson. Med.* **39:** 539–550.

Mansfield, P., Chapman, B. L. W., Bowtell, R., Glover, P., Coxon, R., and Harvey, P. R. 1995. Active acoustic screening—Reduction of noise in gradient coils by Lorentz force balancing. *Magn. Reson. Med.* **33:** 276–281.

Mansfield, P., and Pykett, I. 1978. Biological and medical imaging by NMR. *J. Magn. Reson.* **29:** 355–373.

McJury, M., Stewart, R. W., Crawford, D., and Toma, E. 1997. The use of active noise control (ANC) to reduce acoustic noise generated during MRI scanning: Some initial results. *Magn. Reson. Imag.* **15:** 319–322.

Pruessmann, K. P., Weiger, M., Scheidegger, M. B., and Boesinger, P. 1999. SENSE: Sensitivity encoding for fast MRI. *Magn. Reson. Med.* **42:** 952–962.

Roemer, P. B., Edelstein, W. A., Hayes, C. E., Souza, S. P., and Mueller, O. M. 1990. The NMR phased array. *Magn. Reson. Med.* **16:** 192–225.

Shah, N. J., Steinhoff, S., Mirzazade, S., Zafiris, O., Grosse-Ruyken, M.-L., Jäncke, L., and Zilles, K. 2000. The effect of sequence repeat time on auditory cortex stimulation during phonetic discrimination. *Neuroimage* **12:** 100–108.

Thévenaz, P., Ruttimann, U. E., and Unser, M. 1995. Iterative multiscale registration without landmarks. *Proc. IEEE Worksh. Biom. Imag.* 228–231.

Yang, Y., Glover, G. H., van Gelderen, P., Patel, A. C., Mattay, V. S., Frank, J. A. and Duyn, J. H. 1998. A comparison of fast MR scan techniques for cerebral activation studies at 1.5 tesla. *Magn. Reson. Med.* **39:** 61–67.

Waldvogel, D., van Gelderen, P., Muellbacker, W., Ziemann, U., Immisch, I., and Hallett, M. 2000. The relative metabolic demand of inhibition and excitation. *Nature* **406:** 995–998.

de Zwart, J. A., Kellman, P., van Gelderen, P., and Duyn, J. H. 2001. On the potential of sensitivity encoded EPI for BOLD functional brain imaging. *Proc. Int. Soc. Magn. Reson. Med.* **9:** 1217. [Abstract]

de Zwart, J. A., van Gelderen, P., Kellman, P. and Duyn, J. H. Application of sensitivity-encoded echo-planar imaging for blood oxygen level dependent functional brain imaging. *Magn. Reson. Med.*, submitted.